

Regime interpretation of anomalous vortex dynamics in 2D superconductors

Massimiliano Capezzali^(a), Hans Beck^(a) and Subodh R. Shenoy^(b)

^(a) *Institut de Physique, Université de Neuchâtel, Rue A.L. Breguet 1, 2000 Neuchâtel, Switzerland*

^(b) *Condensed Matter Physics Group, International Centre for Theoretical Physics, 34100 Trieste, Italy*

Low-frequency dynamic impedance ($\sigma^{-1}(\omega, T) \equiv (\sigma_1 + i\sigma_2)^{-1}$) measurements on Josephson junction arrays with finite vortex screening length ξ , found that $\sigma_1 \sim |\log \omega|$, $\sigma_2 \sim \text{constant}$. This implies anomalously sluggish vortex mobilities $\mu_V(\omega) \sim \sigma_1^{-1}$, and is in conflict with general dynamical scaling expressions that yield, for low- ω , $\sigma_1 \rightarrow \xi^2$ and $\sigma_2 \rightarrow 0$. We calculate : a) $\sigma(\omega, T)$ by real-space vortex scaling; b) $\mu_V(\omega)$ using Mori's formalism for a screened Coulomb gas. We find, in addition to the usual critical (large- ω) and hydrodynamic (low- ω) regimes, a new intermediate-frequency scaling regime into which the experimental data fall. This resolves the above mentioned conflict and makes explicit predictions for the scaling form of $\sigma(\omega, T)$, testable in SNS and SIS arrays.

PACS numbers: 74.50.+r, 05.90.+m, 74.60.Ge

The dynamic conductivity of superconductors $\sigma(\omega, T) \equiv \sigma_1 + i\sigma_2 \equiv |\sigma|e^{i\phi_\sigma}$, including high- T_C materials and Josephson junction arrays (JJA), has been the focus of much recent interest [1,2,3,4]. Dynamical scaling forms, $\sigma = \xi^{2+z-d} S_\pm(Y^{-1})$, $\phi_\sigma = \Phi(Y^{-1})$ were proposed by Fisher et al. [1] and Dorsey [2], where z is the dynamic exponent, and $Y \sim 1/\omega\xi^z$. The results apply [1,2] also for the vortex-unbinding Kosterlitz-Thouless (KT) transition in $d = 2$ [5], ξ being the vortex screening length. The scaling functions Φ_σ and S_+ (S_-) have well-defined limits in the hydrodynamic ($Y \gg 1$) and critical ($Y \ll 1$) regimes, e.g. $\sigma_1 \rightarrow \xi^2$, $\sigma_2 \rightarrow 0$ in the $Y \rightarrow \infty$, dc limit. 2D JJA's [6] are clean, controllable 2D superconductors, and should be ideal systems to display the universal dynamic scaling behaviour and limits.

Remarkably, however, low-frequency dynamic impedance (σ^{-1}) measurements [4] on 2D SNS triangular-lattice JJA's with a (field-induced) vortex screening length ξ , find $\sigma_1 \sim |\ln \omega|$, $\sigma_2 \sim \text{constant}$, in conflict with dynamic scaling limits. This also implies anomalously sluggish low-frequency vortex mobilities, $\mu_V(\omega) \sim \sigma_1^{-1} \sim 1/|\ln \omega|$ going to zero for $\omega \rightarrow 0$. σ is related to the dynamic dielectric function $\epsilon(\omega)$: $\sigma \sim iY/\epsilon(\omega)$. Surprisingly, Minnhagen's phenomenology (MP) for $\epsilon(\omega)$, described below, and related simulations support this anomalous behaviour, but understanding the apparent breakdown of dynamical scaling, in the very arena where one might expect its clear verification, is of central importance.

In this Letter, we reconcile these results, by a "regime interpretation" [8] defined by the ratio $Y = (r_\omega/\xi)^2$ of the (squares of the) frequency-dependent diffusive probe length [9] $r_\omega = \sqrt{\Gamma_0/\omega}$ and the screening length ξ . Here, Γ_0 is a junction-determined phase diffusion rate, the lattice constant is unity, and we consider weak screening and probes over several lattice constants : $\xi \gg 1$, $r_\omega \gg 1$. We a) recalculate $\sigma(\omega, T)$ by a real-space scaling [10], with an improved treatment of intermediate-

scale screening; b) evaluate the vortex mobility μ_V using Mori's formalism for a screened Coulomb gas [11]. Three probe-scale regimes emerge. I) Probing free-vortex scales ("low" frequencies) $r_\omega \gg \xi$, in a "hydrodynamic" region, Drude behaviour with the correct [1,2] dc conductivity, $\sigma_1(\omega \rightarrow 0, T) \sim \xi^2$, is recovered. II) At intermediate scales/frequencies, $r_\omega \lesssim \xi$, in a new "precritical" region, MP-like behaviour, $\sigma_1 \sim |\log \omega|$ is found. III) Probing bound pair-scales ("high" frequencies) $r_\omega \ll \xi$ in a "critical" region extending from just above T_{KT} to $T = 0$, a scale-dependent vortex damping $\sim \sigma_1 \sim (r_\omega/\ln \omega)^2 \sim (\omega(\ln \omega)^2)^{-1}$ is found, corresponding to large pairs moving in a logarithmically interacting viscous medium of smaller pairs. The results of $\omega \rightarrow 0$, $T \rightarrow T_{KT}^+$, thus depend on the order of the limits. The ratio $R_\sigma = \sigma_1(\omega, T)/\sigma_2(\omega, T) \equiv \cot \phi_\sigma$ at $Y = 1$ interpolates between Drude ($R_\sigma = 1$) and MP ($R_\sigma = 2/\pi$) signatures [7], as ω increases from zero, or T increases from T_{KT}^+ . As a satisfying byproduct of calculation a), the MP-like expressions emerge as approximations to the σ/ξ^2 scaling function, valid in regime II. Calculation b) demonstrates that the general results are independent of the details of JJA dynamics, and depend only on Coulomb gas screening properties. Local spin-wave damping mechanisms specific to SNS arrays [11,12] could play an additional role in producing anomalous behaviour, widening regime II. But both SNS and SIS arrays should show all three regimes in principle, with different relative sizes of regimes I and II, coming from very general considerations.

Two different physical circumstances yield a non-zero free vortex density, and thus finite ξ : i) For zero external flux, and $T > T_{KT}$, $\xi^{-1} = \xi_+^{-1}(T) \sim e^{-(T-T_{KT})^{-1/2}} \neq 0$ above transition, $T > T_{KT}$; while $\xi^{-1} = 0$ for $T < T_{KT}$. ii) Flux-induced vortices of concentration $f \ll 1$ [4] (too dilute to form a stable lattice) can form a one-component plasma with a screening length ξ , given by the Debye ex-

pression $\xi^{-1} = \xi_D^{-1}(f) = (4\pi^2 f/\bar{T})^{1/2} \neq 0$, corresponding to "above transition" for any T .

We now sketch the MP ideas [7], originally developed to describe $\sigma(\omega, T)$ structures at $T = T_\omega > T_{KT}$, where $\xi_+(T_\omega) = r_\omega$. The zero-wavevector conductivity $\sigma(\omega, T)$ is proportional to the corresponding (inverse) dielectric constant: $\sigma(\omega, T)/\sigma_0 K_0 \xi^2 = iY [\varepsilon_V(k=0, \omega, T)]^{-1}$, where σ_0 is a conductivity scale and K_0 the bare vortex coupling. In MP, the real part $\Re(\varepsilon_V(k=0, \omega, T)^{-1})$ of this zero-wave-vector dynamic function is approximated by the zero-frequency static function, $\Re(\varepsilon_V(k, \omega=0, T)^{-1})$, evaluated at the probe scale, $k = r_\omega^{-1}$. The imaginary part, $\Im(\varepsilon_V(k=0, \omega, T)^{-1})$ is found from the Kramers-Kronig (KK) relations, that produce a $\ln Y$ dependence. Thus [7], with $\varepsilon_V(k, \omega=0, T)^{-1} = \bar{k}^2/(\bar{k}^2 + \xi^{-2})$:

$$\frac{\sigma_2}{\sigma_0 K_0 \xi^2} = \frac{Y}{Y+1}, \quad \frac{\sigma_1}{\sigma_0 K_0 \xi^2} = \frac{2Y^2 \ln Y}{\pi Y^2 - 1}. \quad (1)$$

At $Y = 1$, $R_\sigma = 2/\pi$ (i.e. $\phi_\sigma = \arctan(\pi/2)$), an MP signature. The dynamical scaling limits [1,2] in the $Y \ll 1$ critical regime, both above and below T_{KT} , are $\sigma_1 \sim \sigma_2 \sim 1/\omega$ (independent of ξ), $\Phi_\sigma = \pi/2$. In the $Y \gg 1$ hydrodynamic regime, for $T > T_{KT}$ ($T < T_{KT}$), one finds $\sigma_1 \sim \xi^2$, $\sigma_2 \sim 0$, $\Phi_\sigma \sim 0$ ($\sigma_1 \sim \delta(\omega)$, $\sigma_2 \sim 1/\omega$). Eqn. (1) for MP has very different limits, however: $\sigma_1 \sim \xi^2 Y^2 |\ln Y|$, $\sigma_2 \sim 1/\omega$ for $Y \ll 1$; and $\sigma_1 \sim \xi^2 |\ln Y|$, $\sigma_2 \sim \xi^2$ for $Y \gg 1$. (Note that the $Y \gg 1$ limit, for $\xi = \xi_+(T)$ fixed, $\omega \rightarrow 0$, implies infinite dc conductivity, above T_{KT}). We now outline our two complementary calculations, with details elsewhere [8], showing that MP-like behaviour emerges in an intermediate regime II, rather than in the scaling form regimes I, III.

(A) REAL-SPACE VORTEX SCALING AND $\sigma(\omega, T)$

The total (dimensionless) JJA bond current $I_{\mu i}^{tot}$ ($\mu=x, y$ directions) is a sum of Josephson or super- ($\sim \sin \Delta_\mu \theta_i$), phase-slip or normal- ($\sim \Delta_\mu \dot{\theta}_i$) and noise-currents, and is conserved at every 2D lattice site i . If we ignore capacitive charge build-up on grains,

$$\sum_\mu \Delta_\mu I_{\mu i}^{tot} = \sum_\mu \Delta_\mu [\bar{T}^{-1} \sin(\Delta_\mu \theta_i - \dot{A}_{\mu i}(t)) + \nu_0^{-1} (\Delta_\mu \dot{\theta}_i - \dot{A}_{\mu i}(t)) + f_{\mu i}(t)] = 0. \quad (2)$$

Here, $\nu_0 \equiv (2eR_J I_J / \hbar) \bar{T} \equiv \Gamma_0 \bar{T}$, $\bar{T}^{-1} \equiv (\hbar I_J / 2ek_B T)$, and I_J , R_J are the junction critical current and RSJ model effective shunt resistance [10,13], for the SNS/SIS array. The random noise current obeys $\langle f_{\mu r}(t) f_{\mu' r'}(t') \rangle = (2/\nu_0) \delta_{\mu\mu'} \delta_{rr'} \delta(t-t')$. The JJA grain phases are $-\pi < \theta_i \leq \pi$, and the external transverse vector potential $A_{\mu i}(t) = A_{\mu i}(\omega) e^{-i\omega t}$ is weak. Inverting the Laplacian

$\bar{\Delta}^2$ on $\dot{\theta}_i$, the Langevin dynamics equation for the phase is [10,14]:

$$\dot{\theta}_r = - \sum_{r'} \tilde{G}_{rr'} \left[\nu_0 \frac{\partial \beta H}{\partial \theta_r} + \hat{F}_{r'}(t) \right], \quad (3)$$

where $\beta H = -\frac{1}{\bar{T}} \sum_{\mu, r} \cos(\Delta_\mu \theta_r - A_\mu(t))$, $\tilde{G}_{rr'} = G_{rr'} - G_{rr}$ is the 2D lattice Green's function (with singular part subtracted), and $\langle \hat{F}_r(t) \hat{F}_{r'}(t') \rangle = 2\nu_0 \tilde{G}_{rr'} \delta(t-t')$.

The dynamic conductivity calculation [10] yields $\sigma_{\mu r, \mu' r'} \equiv \bar{\sigma}_{\mu r, \mu' r'} + \tilde{\sigma}_{\mu r, \mu' r'}$. Here, $\bar{\sigma}$ is the usual superfluid response, that at long wavelengths is $(\bar{\sigma}/\sigma_0) = \pi K_\infty \Gamma_0 \delta(\omega) + iK_\infty (\Gamma_0/\omega)$. With $\langle \rangle_0$ denoting an average with weight $P_0 = e^{-\beta H(\Delta\theta - A(t))}$, $\tilde{\sigma}$ can be written as:

$$\frac{\tilde{\sigma}_{\mu r, \mu' r'}}{\sigma_0} \sim \bar{T}^{-2} \int_0^\infty e^{i\omega t} \langle \sin \Delta_\mu \theta_r e^{-\hat{L}_0 t} \sin \Delta_{\mu'} \theta_{r'} \rangle_0 dt. \quad (4)$$

As before [10], we extract vortices by a dual transform, do a gaussian truncation on spin waves, and find that the effect of the Fokker-Planck "propagator" $e^{-\hat{L}_0 t}$ is to produce a correlation angle decay as $e^{-\Gamma_0 t}$. The correlation $\tilde{\sigma}_{\mu r, \mu' r'}$ can be expressed as the projection (through derivatives) of the vortex partition "generating function", with separated "test charges" at μr and $\mu' r'$. Doing the time integral in Eqn. (4), the $e^{-\Gamma_0 t}$ factors lead to a "test-charge" $(i\omega/\Gamma_0)/(1-i\omega/\Gamma_0)$ at $\mu' r'$ in the partition function. The logarithmic potential, $\bar{\Delta}^2 U_0(R/a) = +2\pi \delta_{\vec{R}, \vec{0}}$ and dipolar ($\xi^{-1} = 0$) scaling equations [5] can be generalized [8] to include weak ($\xi^{-1} \ll 1$) monopolar screening of a , $a + da$ dipole-binding, approximated by a potential $\bar{\Delta}^2 U(R/a) = +2\pi g_l \delta_{\vec{R}, \vec{0}}$. Real-space integration of pairs of separation a , $a + da$ can then be done, as usual [5], producing the renormalized coupling K_l that obeys KT scaling equations. Since vortex damping is across the junctions in the array, it is scale-dependent, $\Gamma_0 \rightarrow \Gamma_l \equiv \Gamma_0/a^2$ ($z = 2$), where $a \equiv e^l$, so the frequency-dependent test charge is $(i\omega a^2/\Gamma_0)/(1-i\omega a^2/\Gamma_0)$ [13]. After projection, this provides a dynamic Drude factor, at scale $a \equiv e^l$, that weights the incremental, (static) scaling contributions, $d(K_l g_l)$. The KK relations are thus automatically satisfied.

With a partial integration, the long-wavelength conductivity $\tilde{\sigma}(\omega)$ is then, finally, an integral over all pair contributions, with a range of length (and time) scales:

$$\frac{\tilde{\sigma}(\omega)}{\sigma_0 \xi^2} = Y \int_0^\infty dl K_l g_l \left[\frac{d}{dl} \frac{(a/r_\omega)^2}{1 - i(a/r_\omega)^2} \right]. \quad (5)$$

For $a \ll 1$, $g_l \simeq 1$, and for $a \gg 1$, g_l is the Debye dielectric constant $q^2/(q^2 + \xi^2)$ at a scale $q \sim a^{-1}$: $g_l \simeq (1 + (a/\xi)^2)^{-1}$. The dominant monopole effect on $\sigma(\omega)$ is the explicit g_l factor, representing a scale-dependent reduction of far-off fields, as seen by a , $a + da$ dipoles.

There is a smooth cross-over from dipolar ($a \ll \xi$, regime III) to monopolar ($a \gg \xi$, regime I) screening with probes $r_\omega \sim a$, and with mutual ($a \sim \xi$, regime II) screening in between. Previously, we had matched regime I/III behaviour directly [10], effectively taking g_l to be a step function, and suppressing the intermediate regime. For external free-vortex screening ($\xi = \xi_D(f)$), $g_l = 1/(1 + (a/\xi)^2)$ throughout.

Changing variables in Eqn. (5), $a/\xi \rightarrow a$ we see $\tilde{\sigma}(\omega, T)$ is a function of Y , with only logarithmic deviations $\sim l_\xi \equiv \ln \xi$, from the limits of the integral and in $K_l \rightarrow K_{l+l_\xi}$. For $\xi \propto \xi_D(f) \sim \sqrt{f}$, this implies a quasi-universality [1] in $Y \sim f/\omega$, as found [4]. The imaginary part $\tilde{\sigma}_2$ of Eqn. (5) has a function peaked at $a^2/\xi^2 = Y$ in square brackets, multiplying a roll-off function. By rapid roll-off and sharp-peaking estimates, the total σ_2 is estimated as ($l_\omega \equiv \ln r_\omega$) :

$$\frac{\sigma_2}{\sigma_0 \xi^2} \approx Y \left[K_{l\xi} \frac{Y^{-2}}{1+Y^{-2}}, K_{l\omega} \frac{Y^{-1}}{1+Y^{-1}}, K_{l\omega} \right], \quad (6)$$

in the regimes I, II, III respectively, or $Y \gg 1$, $Y \leq 1$, $Y \ll 1$. Note in regime III, the ξ^2 factor cancels, and [10] $\sigma_2/\sigma_0 \approx K_{l\omega}/\omega$ with the correct superfluid kinetic inductance limit K_∞/ω , for $T < T_{KT}$, $\omega \rightarrow 0$. The real part of the total conductivity, apart from the $\delta(\omega)$ term, (using KK relations in regime II, where the integral is harder to estimate) is :

$$\frac{\sigma_1}{\sigma_0 \xi^2} \approx \left[\frac{K_{l\xi}}{1+Y^{-2}}, \frac{2 K_{l\omega} \ln Y}{\pi (1-Y^{-2})}, -\frac{1}{2} \frac{dK_{l\omega}}{dl_\omega} \frac{\arctan Y^{-1}}{Y^{-1}} \right] \quad (7)$$

in regimes I, II, III respectively. The σ/ξ^2 results of Eqns. (6) and (7) agree with the scaling limits [1,2] of $S_\pm(Y^{-1})$ and $\phi_\sigma(Y)$ in regimes I, III. In regime II, with dipolar screening neglected ($K_{l\omega} \rightarrow K_0$), σ/ξ^2 is of the MP form, Eqn. (1). With [5] $K_l \sim K_\infty + l^{-1}$ in regime III, $\sigma_1/\sigma_0 \sim (\Gamma_0/\omega)/l_\omega^2$ for all $T < T_{KT}$ reflecting the KT "critical line", in the dynamics; the phase angle [1,2] $\phi_\sigma = \arctan(\sigma_2/\sigma_1) \rightarrow \pi/2$, as $\omega \rightarrow 0$.

(B) COULOMB GAS VORTEX DYNAMICS

It is important to directly calculate the Coulomb gas vortex "charge" mobility [11] (for $\xi^{-1} \neq 0$) in a way that is manifestly independent of the details [13] of JJA dynamics, but shows the two frequency regimes I and II (since dipolar screening is not included, regime III will not appear). The overdamped equation of motion for a charge +1 is $\Gamma_V \dot{\vec{R}}_l = -\sum_{j \neq i} e_j \vec{\nabla} V(\vec{R}_i - \vec{R}_j)$, where the potential between charges ($e_j = \pm 1$) in Fourier space is $V(\vec{q}) = (\vec{q}^2)^{-1}$ and Γ_V is a friction coefficient. We use Mori's formalism [11,15], to relate $\mu_V(\omega)$ to the correlation function $\Phi_{\rho\rho}(\vec{q}, \omega)$ for the vortex charge density

$\rho(\vec{R}) = \sum_i e_i \delta(\vec{R} - \vec{r}_i)$. The inverse mobility of a given particle or effective viscosity function is the sum of the bare friction coefficient and a contribution that is related to the forces from all other particles :

$$\mu_V^{-1}(\omega) = \Gamma_V \left[1 + (k_B T)^{-1} \sum_{\vec{q}} |\vec{q} V(\vec{q})|^2 \Phi_{\rho\rho}(\vec{q}, \omega) \right]. \quad (8)$$

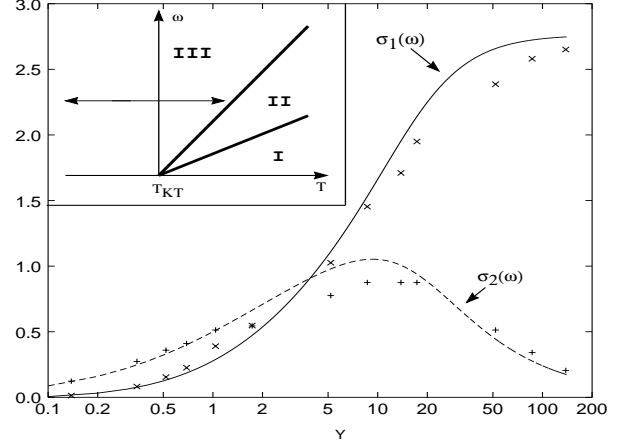


FIG. 1. Real and imaginary parts of the conductivity $\sigma/\sigma_0 \xi^2$ versus $Y \equiv \Gamma_0/\omega \xi^2$, in a linear-log plot, from Eqn. (5). Here ξ is the vortex screening length and $(\Gamma_0/\omega)^{1/2}$ the probe length r_ω . The +, x symbols are experimental data points [4]. Inset : regimes I, II, III in a schematic frequency-temperature diagram, with $r_\omega^{-1} = \xi_+^{-1}(T)$ defining the II/I boundary.

In order to evaluate $\Phi_{\rho\rho}(\vec{q}, \omega)$ we make the usual approximations [11] (neglect of the "Mori projector" and decoupling higher correlations in terms of $\rho(\vec{q})$ and $n(\vec{q})$, the number density Fourier component). One obtains :

$$\Phi_{\rho\rho}(\vec{q}, \omega) = \frac{S_\rho(\vec{q})}{i\omega + \frac{k_B T (\vec{q}^2 + \xi^{-2})}{\mu_V(\omega)}}. \quad (9)$$

Here, $S_\rho(\vec{q})$ is the static (charge) structure factor. Eqns. (8) and (9) determine $\mu_V(\omega)$ self-consistently, but we solve to leading order, replacing μ_V^{-1} in Eqn. (9) by the zeroth order Γ_V . An approximate form is chosen for $S_\rho(\vec{q}) = \frac{k_B T \vec{q}^2}{2\pi n_0 e^2} \Theta(|\vec{q}_1| - |\vec{q}|) + \Theta(|\vec{q}| - |\vec{q}_1|)$ (n_0 being the total density of the charges and $|\vec{q}_1|$ a cut-off, corresponding to the first maximum in $S_\rho(\vec{q})$). We find :

$$\mu_V^{-1}(\omega) = \Gamma_V \left[1 + \frac{\pi J}{k_B T} \ln \left(1 + \frac{\vec{q}_1^2}{i\omega \Gamma_V + \xi^{-2}} \right) \right]. \quad (10)$$

neglecting at first the second term of $S_\rho(\vec{q})$. The Coulomb-gas dielectric function of the system is related to the charge mobility μ_V and to the bound-pair part of the dielectric function by [11] $\varepsilon(\omega) = \varepsilon_B + i e^2 n_0 \mu_V(\omega)/\omega$.

We now present the results. Fig. 1 shows, from Eqn. (5), $\sigma_2/\sigma_0 \xi^2$, as well as $\sigma_1/\sigma_0 \xi^2$ (that for small ω is

essentially $\mu_V^{-1}(\omega)$ the inverse vortex mobility, or vortex viscosity) versus the logarithmic scaled frequency or temperature variable, $\ln Y^{-1}$. The experimental data [4] have been obtained for field-induced free vortices ($\xi^{-1} = \xi_D^{-1}(f) \neq 0$) for which regime III is absent and $g(l) = (1 + (a/\xi)^2)^{-1}$, $\forall a$. Thus the coupling K_l should scale to zero for $l \rightarrow \infty$ (corresponding to $T > T_{KT}$ in the zero field case). We use the simple form $K_l = K_0 \Theta(l_{max} - l)$, and use l_{max} as fitting parameter. A good fit is obtained for $l_{max} = 4.81$, that is on the order of the l -value for which the linearized scaling equations [5] yield a vanishing K_l . $\sigma_1(\omega)$ clearly matches Drude behaviour for regime I, $Y \gg 1$. The "intermediate" regime, $Y \lesssim 1$, with MP dependence $\sim \ln Y$ is seen to be fairly large. The experimental [4] data points for SNS arrays, shown in Figs. 1,2, fall in regimes I and II. Very low frequency data are not unequivocal and are not shown. Typically [4], $\Gamma_0 \sim 300$ Hz, ω varies from ~ 10 Hz to ~ 10 kHz, for $R_J \sim 2m\Omega$ (SNS arrays) and $I_J \sim 100$ nA, and $\xi(f) \sim 3.1$ for $f = 0.001$, so Y goes from ~ 0.1 to ~ 200 .

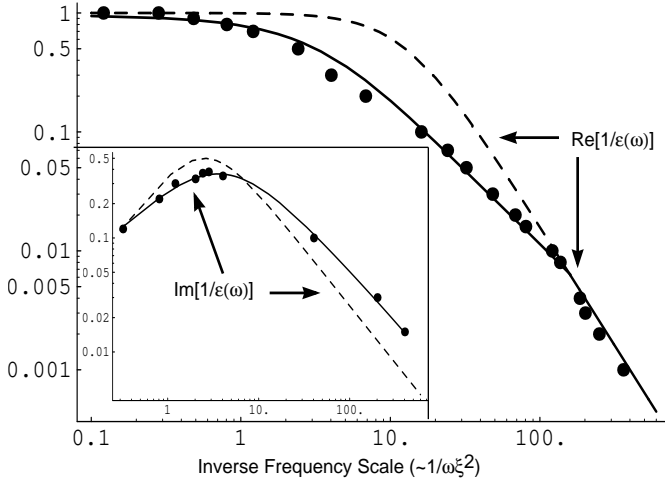


FIG. 2. Real and, in the inset, imaginary parts of $1/\varepsilon(\omega)$ versus an inverse frequency scale $\sim Y$, in a log-log plot. The constant-mobility ($\mu_V^{-1}(\omega) = \Gamma_V$) Drude limit is represented by the dashed line, while the solid line is the result of our calculation b). The experimental results of Ref. [4] are given by the dots.

Fig. 2 shows the dielectric function $\varepsilon(\omega)$ (obtained through Eqns. (8) and (9), by using the full form of $S_\rho(\vec{p})$) as a function of Y . One again clearly recognizes two-frequency regimes (I and II), separated by a crossover frequency $\omega_{cross} \approx (n_0 \xi^2)^{-1}$. For $\omega > \omega_{cross}$, $\Re(1/\varepsilon(\omega))$ varies like $|\omega|$ as in Minnhagen's regime II, whereas for $\omega < \omega_{cross}$, it varies like ω^2 , as in Drude's regime I. Moreover, we have verified for both methods, that the ratio R_σ at $Y = 1$ varies between the Drude ($R_\sigma = 1$) and MP ($R_\sigma = 2/\pi$) signatures [8].

Regime III is not reached for the Y -values shown in Fig. 1, but for SIS arrays, R_J is orders of magnitude higher,

so the critical behaviour might be more clearly seen. Below T_{KT} , or more generally, for $Y \ll 1$, one has effective damping coefficients $\eta_V \sim \sigma_1$ due to bound pairs, rather than free-vortex inverse mobilities, and $\sigma_1 \sim 1/\omega l_\omega^2$. This is consistent with simulations of driven vortices: there is a velocity-dependent viscosity coefficient, decreasing for larger velocities [16]. Larger oscillating pairs, probed at lower ω , are more sluggish, since they move in a logarithmically interacting viscous medium of smaller pairs.

In conclusion, we have proposed a regime interpretation of anomalous vortex dynamics, based on the ratio of the frequency-dependent probe scale, and the screening length. Both Drude and anomalous vortex dynamics emerge in different regimes, from calculations of the dynamic JJA conductivity and the vortex mobility. This reconciles different results, supports postulated conductivity scaling, and indicates further dynamical avenues to be explored, in simulations and experiments.

It is a pleasure to thank D. Bormann, P. Martinoli and P. Minnhagen for useful conversations, and P. Martinoli for reading the manuscript.

-
- [1] D.S. Fisher et al., Phys. Rev. **43**, 130 (1991);
 - [2] A.T. Dorsey, Phys. Rev. **43**, 7575 (1991); A.T. Dorsey et al., Phys. Rev. **45**, 523 (1992)
 - [3] P. Minnhagen et al., Phys. Rev. Lett. **74**, 3672 (1995).
 - [4] R. Théron et al., Phys. Rev. Lett. **71**, 1246 (1993).
 - [5] J.M. Kosterlitz and D.J. Thouless, J. Phys. C **6**, 1181 (1973); J. Phys. C **7**, 1046 (1974).
 - [6] J.E. Mooij and G. Schön, eds., Physica B+C **157**, (1987); H. A. Cerdeira and S.R. Shenoy, eds., Physica B **222** (1996).
 - [7] P. Minnhagen, Rev. Mod. Phys. **59**, 1001 (1987); M. Wallin, Phys. Rev. B **41**, 6575 (1990); P. Minnhagen and O. Westman, Physica **C220**, 347 (1994); J. Houlrik et al., Phys. Rev. B **50**, 3953 (1994).
 - [8] H. Beck, M. Capezzali, S.R. Shenoy (unpublished).
 - [9] V. Ambegaokar et al., Phys. Rev. B **21**, 1806 (1980).
 - [10] S.R. Shenoy, J. Phys. C **18**, 5143 and 5163 (1985); J. Phys. C **20**, 2479 (1987).
 - [11] H. Beck, Phys. Rev. B **49**, 6153 (1994).
 - [12] S.E. Korshunov, Phys. Rev. B **50**, 13616 (1994).
 - [13] For SNS arrays, in addition to intergrain normal currents described by effective damping ν_0 , there can be grain-to-substrate losses of normal current, incorporated in a generalized TCC dynamics as a local current term $(1/\nu_1)\theta_i$ in Eqn. (2). Here, the local damping rate ν_1 is scale-independent. However, following the argument [10] through, there is, from the $(1/\nu_1)\theta_i$ term, a decay rate in Fourier space $\nu_1 q^2$ that for q^{-1} in a , $a + da$ scales as ν_1/a^2 , like $\nu_0 \rightarrow \nu_0/a^2$. Thus SIS (ν_0 only) and SNS (ν_0, ν_1) arrays should have the same Coulomb-gas dynamics, as supported by calculation b).
 - [14] K.K. Mon and S. Teitel, Phys. Rev. Lett. **62**, 673 (1989).
 - [15] W. Götze, Phil. Mag. B **43**, 219 (1981).
 - [16] T. Hagenaars et al., Phys. Rev. B **50**, 1143 (1994).